



HAL
open science

Main individual and product characteristics influencing in-mouth flavour release during eating masticated food products with different textures: mechanistic modelling and experimental validation

Marion M. Doyennette, Isabelle Deleris Déléris, Gilles Feron, Elisabeth E. Guichard, Isabelle I. Souchon, Ioan-Cristian I.-C. Trelea

► To cite this version:

Marion M. Doyennette, Isabelle Deleris Déléris, Gilles Feron, Elisabeth E. Guichard, Isabelle I. Souchon, et al.. Main individual and product characteristics influencing in-mouth flavour release during eating masticated food products with different textures: mechanistic modelling and experimental validation. *Journal of Theoretical Biology*, 2014, 340, pp.209-21. 10.1016/j.jtbi.2013.09.005 . hal-00939546

HAL Id: hal-00939546

<https://hal.science/hal-00939546v1>

Submitted on 11 Jul 2017

HAL is a multi-disciplinary open access archive for the deposit and dissemination of scientific research documents, whether they are published or not. The documents may come from teaching and research institutions in France or abroad, or from public or private research centers.

L'archive ouverte pluridisciplinaire **HAL**, est destinée au dépôt et à la diffusion de documents scientifiques de niveau recherche, publiés ou non, émanant des établissements d'enseignement et de recherche français ou étrangers, des laboratoires publics ou privés.

1 **Main individual and product characteristics influencing in-mouth flavour release during**
2 **eating masticated food products with different textures: mechanistic modelling and**
3 **experimental validation**

4 M. Doyennette^{a, b}, I. Déléris^{a, b*}, G. Féron^{c, d, e}, E. Guichard^{c, d, e}, I. Souchon^{a, b}, I. C. Tréléa^{a, b}

5 ^aINRA, UMR 0782, F-78850 Thiverval Grignon, France. isabelle.delegeris@grignon.inra.fr;
6 isabelle.souchon@grignon.inra.fr

7 ^bAgroParisTech, UMR 0782, F-78850 Thiverval Grignon, France.
8 cristian.trelea@agroparistech.fr

9 ^cINRA, UMR1324 Centre des Sciences du Goût et de l'Alimentation (CSGA), F-21000
10 Dijon, France. gilles.feron@diijon.inra.fr; elisabeth.guichard@diijon.inra.fr

11 ^dCNRS, UMR6265 CSGA, F-21000 Dijon, France

12 ^e Université de Bourgogne, UMR CSGA, F-21000 Dijon, France

13

14 **Running title:** Modelling release from masticated foods

15

*Correspondence to be sent to: Isabelle Déléris, UMR 0782, 78850 Thiverval Grignon, France, isabelle.delegeris@grignon.inra.fr; tel: +33 (0)1 30 81 54 39; fax: +33 (0)1 30 81 55 97

Highlights:

- The developed model properly describes aroma release from masticated foods
- The mechanistic model includes both physiological and physical mechanisms.
- The most influential parameters for the intensity and the dynamics of the release were identified.
- The modelling approach highlighted aroma retention by lubricated mucosa.

16 **Abstract**

17 A mechanistic model predicting flavour release during oral processing of masticated foods
18 was developed. The description of main physiological steps (product mastication and
19 swallowing) and physical mechanisms (mass transfer, product breakdown and dissolution)
20 occurring while eating allowed satisfactory simulation of *in vivo* release profiles of ethyl
21 propanoate and 2-nonanone, measured by Atmospheric Pressure Chemical Ionization Mass
22 Spectrometry on ten representative subjects during the consumption of four cheeses with
23 different textures. Model sensitivity analysis showed that the main parameters affecting
24 release intensity were the product dissolution rate in the mouth, the mass transfer coefficient
25 in the bolus, the air-bolus contact area in the mouth and the respiratory frequency. Parameters
26 furthermore affecting release dynamics were the mastication phase duration, the velopharynx
27 opening and the rate of saliva incorporation into the bolus. Specific retention of 2-nonanone
28 on mucosa was assumed to explain aroma release kinetics and confirmed when gaseous
29 samples were consumed.

30 **Keywords:** dynamic model; aroma compounds; food oral processing; physiology; mass
31 transfer

32

33 **1. Introduction**

34 The release of aroma compounds from food products during eating is a key step for their
35 perception and ultimately for the acceptance of the product by the consumer. Food oral
36 processing is complex [1] and flavour release induced by this processing depends on both the
37 physiology and experience of subjects and on product properties. To identify what are these
38 main properties explaining flavour release, it is necessary to develop an approach allowing the
39 dissociation of mechanisms occurring during food oral processing. Mathematical modelling
40 can help improving the understanding of the limiting mechanisms by pointing out the most
41 important parameters related to the product and to the individual and allowing quantitative
42 predictions of release dynamics. Therefore, models can help design the food products in a
43 rational way, possibly targeted towards particular consumer groups such as young children,
44 elderly or people with specific disorders.

45 The mechanistic modelling of aroma compound release during food consumption allows one
46 to calculate, from known physical laws, the amount of aroma compounds transferred over
47 time in each anatomical compartment involved during food oral processing (mouth, nasal
48 cavity, pharynx).

49 The first mechanistic models have focused on predicting the release of aroma compounds
50 from a two-phase emulsion (water, oil) in contact with gas [2]. They were based on physico-
51 chemical principles governing the release of volatile molecules from a food matrix: (i) the
52 mass conservation of volatile compound, (ii) the mass transfer at the emulsion-gas interface
53 (interfacial penetration theory), (iii) equilibrium properties at the emulsion-gas interface [3].

54 First-order chemical kinetics have also been included in some models to describe reversible
55 interactions between aroma compounds and non-volatile compounds such as macromolecules
56 [2]. However, these first models are not really representative of *in vivo* phenomena because
57 the geometry of the system (surfaces and volumes) is assumed constant (which is not the case

58 during food consumption) and they do not consider dynamic phenomena such as the dilution
59 with salivary flow or the cyclic breathing of the subject. In addition, some of these models do
60 not include any comparison with experimental data release [2].

61 Further development of these pioneering models has led to a better representation of *in vivo*
62 conditions occurring during food consumption, by including notably parameters related to
63 individual physiology, such as salivary flow, periodic breath, etc. [4, 5]. In addition, one of
64 the major improvements in these models was to consider the aroma persistence phenomenon
65 i.e. aroma release from bolus deposit covering the pharyngeal mucosa after swallowing. These
66 models showed the relative roles of product and consumer characteristics and were validated
67 against experimental data.

68 The first model including physiological data was proposed by Normand *et al.* [4] in the case
69 of liquid products and highlighted two main release regimes: (i) release due to equilibrium
70 batch extraction (only pertinent for few breaths after swallowing) and (ii) release from
71 lubricated mucosa (persistence phenomena). In the case of semi-liquid food, the most
72 comprehensive model to date is the one developed by Tréléa *et al.* [6] and further developed
73 by Doyennette *et al.* [7] coupling aroma release in the mouth and in the pharynx.

74 Mechanistic models describing aroma release from masticated foods are far less available in
75 the literature, mostly because of the difficulty to understand the complex mechanisms which
76 are involved during the consumption of those foods. Compared to liquid products, mass
77 transfer occurs through several interfaces (product/saliva, saliva/air) in “solid” matrices
78 (needing mastication) [8, 9]. Also, additional phenomena have to be considered: product
79 dissolution and melting due to intraoral manipulations (chewing, saliva incorporation,
80 warming) and the generation of a dynamic exchange interface between product and saliva.

81 Existing models describing aroma release from solid food are not complete since they do not
82 take breathing into account [5, 10]. Furthermore, the assumptions used are not always

83 transferable to other types of food matrices and to associated food oral processes than those
84 studied (e.g. candy) or to other consumption patterns (e.g. sucking mechanism studied by
85 Wright *et al.* [5]).

86 Hills and Harrison [10] also highlighted the importance of modelling the variation in the
87 contact surface between the product and saliva, whose change in time plays a central role in
88 the aroma compounds release. In their model, they suggest a multi-fragmentation theory to
89 represent the chewing of a candy (assimilated to a cube). This approach provides a law of
90 time change in the contact surface between product and saliva, using only two parameters: the
91 number of bites and the duration of chewing. One might expect, however, that chewing real
92 products, like cheeses for instance, will not always produce cubes and multiply the area by a
93 factor of 2 after each bite. Other studies have also investigated the fragmentation of solids
94 placed in the mouth under the action of chewing. The degree of fragmentation of a food can
95 be determined by different types of experimental measurements such as the analysis of
96 particle size distribution in the bolus [11]. These experimental data allow the determination of
97 the laws of fragmentation depending on the type of food: deterministic analytic laws of
98 product fragmentation over time [12], or probabilistic laws [8, 13-15]. While these approaches
99 can be very comprehensive, they have several limitations. For example, some of them require
100 complex experimental protocols that are difficult to implement (bolus spitting after a variable
101 number of bites). Other approaches need the determination of many parameters (such as the
102 number of chews, the number or the size of food particles after each chew, etc...), usually
103 unknown, and which may depend on the product and/or on the individual.

104 From this literature review, it appears that modelling the release of aroma compounds during
105 solid food consumption remains a challenging task and that the results of published studies
106 are difficult to extrapolate to other experimental conditions. In this context, the present study
107 proposes a model simulating the release of aroma compounds, applicable to different food

108 matrices and different individuals with a wide range of physiological characteristics. With this
109 mechanistic model, our main objective was to understand the mechanisms and parameters
110 governing the release of aroma compounds during the intra-oral manipulation and swallowing
111 of “solid” food (needing chewing). To do so, simulations issued from the model were
112 compared to *in vivo* release data of two aroma compounds, measured by atmospheric pressure
113 chemical ionization mass spectrometry (APCI-MS) on ten panelists, during the consumption
114 of four sorts of cheese, varying in composition and texture. Model assumptions are presented
115 and their validity is discussed.

116 **2. Mathematical modelling of *in vivo* aroma compound release**

117 2.1. Principles of the model

118 The aroma release model described in this study applies to food products requiring
119 mastication. It is an extension of the model developed for liquid and semi-liquid foods by
120 Doyennette *et al.* [7]. The new insight is the consideration of the mastication process. The
121 global eating process involves several steps shown in figure 1: the initial state of the system
122 (product introduction in mouth), the intra-oral manipulation of the product, which consists in
123 several masticatory cycles, one or more swallowing events and the resting phase (release
124 during the post-mastication stage) which occurs when there is no more product in the mouth.

125 The intra-oral manipulation phase usually lasts until the first swallow. However, in some
126 cases (particularly for firm products), it can extend beyond the first swallow.

127 Similarly to the model of Doyennette *et al.* [7], the present description of the swallowing step
128 includes simultaneous contractions of the oral cavity and of the pharynx, leading to air and
129 product expulsion, followed by relaxation and filling with fresh air. This will cause the
130 expulsion of the bolus formed in the mouth into the pharynx. Each swallowing step leads to
131 the deposit of a small part of the in-mouth liquid phase of the bolus on the pharyngeal walls.

132 A residual amount of the solid part of the bolus remains in the mouth and is chewed again and
133 mixed with saliva in order to form a new food bolus suitable for swallowing.

134 A schematic representation of the four compartments involved in the model design, as well as
135 their connections and the mechanisms responsible for flavour release, are given in figure 2.
136 All variables and parameters of the interconnected compartments required for the model
137 simulation are specified in this figure.

138 Compared to the previous model [7], two main differences can be observed: first, the presence
139 of three instead of two sub-compartments in the mouth (the non-dissolved food product,
140 which is the solid part of the bolus, the liquid phase of the bolus, made of saliva and dissolved
141 food product and the air phase) and secondly, the opening of the velopharynx during chewing,
142 allowing the transport of aroma compounds between the air phases of mouth and pharynx
143 (figure 2).

144 Concerning the food bolus fragmentation under mastication, the particle size distribution in
145 the bolus after each bite has already been described in literature [8, 11, 13-15]. However,
146 these approaches require the knowledge of parameters such as food particle size after each
147 chew, which is difficult to determine experimentally, particularly for pasty products like
148 cheese used in the present study. The relevant parameter for aroma compound release is not
149 the particle size itself, but the contact area between the solid and the liquid phase of the bolus.
150 In this study, we focus on the generation of this area, as previously done in literature [16]. In
151 the following paragraphs, the main differences with the previously published model for liquid
152 products [7] are emphasized.

153 2.2. Mathematical description of mass transfer in mouth during the eating of masticated foods

154 The solid food product placed in the mouth is broken down during intra-oral manipulation.

155 Two concurrent phenomena can occur:

156 • the transfer of aroma compounds from the non-dissolved product into the liquid phase of the
157 bolus,
158 • the melting (dissolution) of the product in the liquid phase of the bolus due to the combined
159 action of the mastication, the saliva incorporation and the warming of the product in the
160 mouth. This also leads to the release of aroma compounds contained in the dissolved product
161 towards the liquid phase of the bolus.

162 In practice, it is very difficult to distinguish between the relative contributions of each
163 mechanism. Moreover, the phenomena of transfer and of dissolution can be described by very
164 similar equations. Considering the studied products (cheeses), we arbitrarily chose to assign
165 the release of aroma compounds into saliva to a single mechanism (dissolution) while being
166 aware that the transfer also contributes to this process.

167 2.2.1. Air/bolus interfacial conditions in the oral cavity

168 Similarly to Doyennette *et al.* [7], the transfer resistance on the air side $1/k_{OA}$ was assumed to
169 be negligible when compared to the transfer resistance on the product side $1/k_{OL}$ (the orders
170 of magnitude of the mass transfer coefficients, representing the reciprocal of the resistances,
171 are 10^{-2} and 10^{-6} m/s respectively [17]).

172 Therefore, the interfacial aroma compound concentration on the liquid bolus side, using the
173 partition conditions at the interface, is given by:

$$174 C_{OAL}^*(t) = \frac{C_{OA}(t)}{K_{OAL}(t)} \quad (1)$$

175 The volatile mass flux between the air and the liquid bolus in the oral cavity ϕ_{OAL} is mainly
176 determined by the resistance located on the bolus side and is given by the difference between
177 the liquid bolus concentration (C_{OL}) and the interfacial concentration (C_{OAL}^*):

$$178 \phi_{OAL}(t) = k_{OL}(t) \times A_{OAL}(t) \times (C_{OL}(t) - C_{OAL}^*(t)) \quad (2)$$

179 2.2.2. Air in the oral cavity

180 In addition to the aroma compound flux from the liquid bolus, the air in the mouth can also
 181 exchange aroma compounds with the air in the pharynx. Jaw movements during mastication
 182 induce velopharynx opening and cyclic air flow between the pharynx and the mouth [18].

183 The variation of aroma concentration in the air in the oral cavity C_{OA} is thus due to the
 184 volatile flux from the liquid food bolus and from the air coming from the pharynx ($Q_{OA} \geq 0$
 185 means that the air flows in the direction shown by the arrow in figure 2):

$$186 \quad V_{OA}(t) \times \frac{dC_{OA}(t)}{dt} = \phi_{OAL}(t) + \begin{cases} Q_{OA}(t) \times (C_{FA}(t) - C_{OA}(t)) & \text{if } Q_{OA}(t) \geq 0 \\ 0 & \text{if } Q_{OA}(t) < 0 \end{cases} \quad (3)$$

187 Little is known on the real change in V_{OA} . It was assumed that the masticatory movements
 188 create a cyclic variation of the air volume V_{OA} around a mean value $V_{OA\ mean}$ as it has been
 189 observed by Matsuo *et al.* [18]. In this case:

$$190 \quad V_{OA}(t) = V_{OA\ mean} + \Delta V_{OA} \times \sin(2 \times \pi \times fr_{opening} \times t) \quad (4)$$

191 Therefore, the air flow rate coming from the mouth Q_{OA} is calculated as follows:

$$192 \quad Q_{OA}(t) = \frac{dV_{OA}(t)}{dt} = 2 \times \pi \times fr_{opening} \times \Delta V_{OA} \times \cos(2 \times \pi \times fr_{opening} \times t) \quad (5)$$

193 It is expected that ΔV_{OA} can be highly variable among individuals, but no quantitative data was
 194 found in the literature. A fair estimation of ΔV_{OA} seems to be 20% of $V_{OA\ mean}$, value which
 195 was used in our model. Based on observations from Matsuo *et al.* [18], we assumed that
 196 $fr_{opening}$ can vary among individuals, within a defined range. We supposed that the highest
 197 opening frequency was coordinated with the masticatory frequency ($fr_{masticatory}$), and that the
 198 lowest opening frequency was coordinated with the respiratory frequency (F_R). This
 199 assumption will be further discussed in the results and discussion section.

200 2.2.3. Product in the oral cavity

201 In line with the assumption of the dissolution rather than transfer mechanism discussed above,
 202 the aroma compound concentration in the solid (undissolved) food product fraction remains
 203 constant in time:

204 $C_{OP}(t) = C_{OP}(0)$ (6)

205 Due to dissolution and fragmentation processes, the volume of the solid food product
 206 decreases over time, while its contact area with the liquid phase of the bolus increases and
 207 then abruptly decreases due to swallowing.

208 The dissolution of the product at a rate v gives the following equation:

209 $\frac{dV_{OP}(t)}{dt} = -v \times A_{OLP}(t)$ (7)

210 Due to fragmentation induced by mastication, the contact area between the solid product
 211 present in the mouth and the liquid bolus increases in time. The exact rate of change of this
 212 contact area is not known for pasty products, like cheeses used in this study. In absence of
 213 more detailed information we assumed that, as long as some solid product is present in the
 214 mouth and a regular mastication behaviour were considered, its contact area with the liquid
 215 bolus evolves linearly over time. This simplifying hypothesis might be refined in the future
 216 based on more detailed studies, however. With this assumption:

217 $\frac{dA_{OLP}(t)}{dt} = \begin{cases} \frac{A_{OLPdeg} - A_{OLPini}}{t_{deg} - t_0} & \text{if } V_{OP}(t) > 0 \\ 0 & \text{if } V_{OP}(t) = 0 \end{cases}$ (8)

218 with the index "*deg*" meaning "at the current deglutition moment", and the index "*ini*"
 219 meaning "at food product introduction in mouth" (at t_0) or "just after the previous
 220 deglutition".

221 2.2.4. Liquid bolus in the oral cavity

222 The liquid bolus compartment has a composition which evolves over time. It is initially
 223 composed of pure saliva, and is progressively flavoured by the addition of dissolved product.
 224 Its volume increases with the addition of saliva (salivary flow) and with the incorporation of
 225 dissolved product, and periodically decreases after swallowing.

226 The volume of the bolus $V_{OL}(t)$ can be thus divided into two parts:

227 $V_{OL}(t) = V_{OS}(t) + V_{OPD}(t)$ (9)

228 In that case, we have:

$$229 \quad \frac{dV_{OS}(t)}{dt} = Q_{OS} \quad (10)$$

230 with $\frac{dV_{OPD}(t)}{dt}$ the product dissolution rate, defined as

$$231 \quad \frac{dV_{OPD}(t)}{dt} = v \times A_{OLP}(t) \quad (11)$$

232 The mass balance for a given aroma compound in the bolus leads to the following equation:

$$233 \quad \frac{dV_{OL}(t) \times C_{OL}(t)}{dt} = \phi_{OLP}(t) - \phi_{OAL}(t) \quad (12)$$

234 with the volatile mass flux ϕ_{OLP} coming from product dissolution:

$$235 \quad \phi_{OLP}(t) = v \times A_{OLP}(t) \times C_{OP}(t) \quad (13)$$

236 The mass flux ϕ_{OAL} is given by the difference between the aroma concentration in the liquid
237 phase of the bolus (C_{OL}) and the interfacial concentration (C^*_{OAL}) (Eq. 2).

238 The properties of the liquid bolus relevant for aroma compound transfer, namely the air/bolus
239 partition coefficient (K_{OAL} , Eq. 1) and the mass transfer coefficient (k_{OL} , Eq. 2) change with
240 the relative fraction of the saliva and dissolved product in the liquid bolus. This dependence
241 was previously established [19] and included in the model simulations.

242 2.3. Mathematical description of aroma release during the pharyngeal step

243 2.3.1. Bolus in the pharynx

244 Phenomena governing flavour release from the bolus in the pharynx are similar to the ones
245 described for liquid products [7].

246 2.3.2. Air in the pharynx

247 The air in the pharynx exchanges aroma compounds with the bolus in the pharynx, and with
248 the other compartments: the mouth (air flow $Q_{OA}(t)$), the nose (air flow $Q_{NA}(t)$) and the
249 trachea (air flow $Q_{TA}(t)$). Compared to the model of Doyennette *et al.* [7], air flows to and
250 from the mouth have been modified (due to the velopharynx opening during mastication). By

251 convention, the air flow rates indicated in figure 2 are positive if they follow the direction of
 252 the arrow. The air balance in the pharynx at any time gives the following relationship:

$$253 \quad Q_{NA}(t) = -Q_{TA}(t) + Q_{OA}(t) \quad (14)$$

254 For the considered aroma compound, the mass balance in the air of the pharynx gives the
 255 equation:

$$256 \quad V_{FA} \times \frac{dC_{FA}(t)}{dt} = \phi_{FAL}(t) + \begin{cases} -Q_{OA}(t) \times (C_{OA}(t) - C_{FA}(t)) & \text{if } Q_{OA}(t) < 0 \\ Q_{NA}(t) \times (C_{NA}(t) - C_{FA}(t)) & \text{if } Q_{NA}(t) \geq 0 \\ Q_{TA}(t) \times (C_{TA}(t) - C_{FA}(t)) & \text{if } Q_{TA}(t) \geq 0 \end{cases} \quad (15)$$

257 2.4. Conditions of the system after each deglutition

258 The deglutition step is very short compared to product residence time in mouth. It is thus
 259 described as quick contraction and relaxation events (figure 1).

260 2.4.1. Product and bolus in the oral cavity after deglutition

261 Aroma compound concentrations in the product and in the bolus are unchanged during
 262 deglutition. The volume of product in the oral cavity just after deglutition (V_{OPdeg+}) decreases
 263 and corresponds to the volume of product just before swallowing (V_{OPdeg-}) multiplied by the
 264 fraction of liquid bolus remaining in the mouth after deglutition (r_L), i.e. :

$$265 \quad V_{OPdeg+} = V_{OPdeg-} \times r_L \quad (16)$$

266 Similarly, the liquid bolus/product contact area in the oral cavity after swallowing is
 267 calculated as:

$$268 \quad A_{OLPdeg+} = A_{OLPdeg-} \times r_L$$

$$269 \quad (17)$$

270 The volumes of saliva (V_{OSdeg+}) and of dissolved product ($V_{OPDdeg+}$) in the oral cavity
 271 decrease after swallowing. We assume that the bolus liquid part (saliva and dissolved product)
 272 is uniformly swallowed. Therefore, we have:

$$273 \quad V_{OSdeg+} = V_{OSdeg-} \times \frac{V_{Salivadeg+}}{V_{OSdeg-} + V_{OPDdeg-}}, \text{ and } V_{OPDdeg+} = V_{OPDdeg-} \times \frac{V_{Salivadeg+}}{V_{OSdeg-} + V_{OPDdeg-}} \quad (18)$$

274 with $V_{Salivadeg+}$ being the volume of saliva usually present in the oral cavity after swallowing.

275 2.4.2. Aroma compound retention by lubricated mucosa

276 To take the reservoir effect of lubricated mucosa into account, additional compartments were
 277 included into the model. We assumed that air in the mouth, in the pharynx and in the nose was
 278 in contact with lubricated mucosa layers within the corresponding compartment. For example,
 279 in the nose, the volatile mass flux ϕ_{NAM} between the air and the mucosa is given by:

$$280 \phi_{NAM}(t) = k_{NM} \times A_{NAM} \times (C_{NM}(t) - \frac{C_{NA}(t)}{K_{NAM}}) \quad (19)$$

281 The mass balance of aroma compound in air contained in nasal cavity leads to:

$$282 V_{NA} \times \frac{dC_{FA}(t)}{dt} = \phi_{NAM}(t) + \begin{cases} Q_{NA}(t) \times (0 - C_{NA}(t)) & \text{if } Q_{NA}(t) \geq 0 \\ Q_{TA}(t) \times (C_{FA}(t) - C_{TA}(t)) & \text{if } Q_{TA}(t) \geq 0 \end{cases} \quad (20)$$

283 and in nasal mucosa:

$$284 V_{NM} \times \frac{dC_{NM}(t)}{dt} = -\phi_{NAM}(t) \quad (21)$$

285 Here, V_{NM} is the volume of lubricated mucosa which is involved in the interaction with the
 286 aroma compound. It can be expressed as

$$287 V_{NM} = e_{NM} \times A_{NAM} \quad (22)$$

288 Similar equations were added in the mouth and in the pharynx to take the effect of the
 289 lubricated mucosa present in these compartments into consideration. In the absence of more
 290 detailed information, the contact area between lubricated mucosa and air was arbitrarily set to
 291 half of the contact area between the bolus and the air in the mouth, as well as in the pharynx.
 292 Little information is available in the literature concerning values to be considered in the
 293 aroma retention model. The contact area between air and lubricated mucosa in the nose A_{NAM}
 294 was set to 160 cm² [20]. In literature, values comprised between 5.6×10^{-5} and 4.8×10^{-1} were
 295 mentioned for air/mucus partition coefficient of butanol and octanol in bullfrog [21]. Thus, a
 296 typical value of 1×10^{-3} was selected here. Concerning the mucosa layer thickness, Shojaei
 297 [22] gave values between 500 and 800 μm in mouth and 100 to 200 μm for the gingival
 298 mucosa. It is expected, however, that the aroma compound will not necessarily have time to

299 diffuse in the whole epithelium thickness, and these values are considered as upper limits for
300 mucosa layer thickness involved in aroma retention.

301 **3. Material and Methods**

302 3.1. Flavoured cheese products

303 Four industrial cheese products (melt-cheese technology) varying in composition and texture
304 (two fat levels and two firmness levels) and flavoured with ethyl propanoate and 2-nonanone
305 were studied [23]. They were coded according to their characteristics, with a combination of
306 letters as following: S or F for Soft or Firm respectively and l or h for low-fat or high-fat
307 respectively.

308 *Panelist selection and their physiological characterization at rest*

309 Ten individuals were selected from a large panel composed of 44 subjects: they were verified
310 to be representative of the whole panel (mean and standard deviation) concerning
311 physiological data, masticatory behavior and APCI-MS release kinetics [23].

312 The volumes of oral, nasal and pharyngeal cavities of subjects were measured with the
313 Eccovision Acoustic Rhinopharyngometer from Eccovision (Sleep Group Solutions, North
314 Miami Beach, FL 33162). A software was developed to calculate automatically the
315 air/product areas of oral and pharyngeal cavities for each individual [7].

316 The tidal volume of each individual was measured with a spirometer (Pulmo System II, MSR,
317 Rungis, France) [23]. The respiratory frequency F_R used in the model was calculated directly
318 from the acetone signal measured by APCI-MS.

319 3.2. In-nose measurements of aroma release by Atmospheric Pressure Chemical Ionization– 320 Mass Spectrometry (APCI-MS) and data processing

321 Aroma release was measured using APCI-MS [23]. For each product, each panelist and for
322 the three replicates, a mean curve and an envelope curve (representing the standard deviation
323 of the replicates) were determined based on the peak lines (curve linking the maxima of

324 aroma release profile) [7]. Release kinetics were divided in two different phases: “phase 1”
 325 corresponded to the chewing phase before the first deglutition and “phase 2” corresponded to
 326 the rest of the chewing phase (if present) and to the resting phase. The end of phase 2 was set
 327 when less than 10% of the maximal intensity was reached. Areas under curve (AUC) were
 328 determined for each phase.

329 3.3. Physiological characterization of individuals during cheese consumption

330 Chewing activity, bolus saliva content and mouth coating were determined for each panelist
 331 as described in Repoux *et al.* [23].

332 It has been demonstrated from various studies [24, 25] that salivary flow during food
 333 consumption is much higher than the salivary flow at rest or artificially stimulated. Therefore,
 334 an average rate of saliva incorporation in the bolus during food product consumption (Q_{OS})
 335 was estimated with the following equation:

$$336 \quad Q_{OS} = \frac{\text{percentage of incorporated saliva} \times \text{amount of food ingested}}{100 \times \text{duration of phase 1}} \quad (23)$$

337 with the amount of food ingested = 6g, and phase 1 being the chewing phase before the first
 338 swallow. The percentage of incorporated saliva (relative to the product) was calculated as
 339 follows, based on moisture content of the initial cheese and of the bolus:

$$340 \quad \text{percentage of incorporated saliva} = \frac{HM_{bolus}}{100 - HM_{bolus}} \times (100 - HM_{cheese}) - HM_{cheese} \quad (24)$$

341 The percentage of incorporated saliva and the duration of phase 1 were determined during two
 342 separate experimental sessions, which can induce biased calculation (the salivary flow rate is
 343 known to vary daily and with the physiological state of the individual). Therefore, the average
 344 rate of saliva incorporation in the bolus during food consumption calculated with Eq. 23 was
 345 only indicative and we preferred to use this parameter as a degree of freedom of the model for
 346 simulations.

347 In this study, neither the frequency nor the displacement amplitude of the soft palate during
 348 food consumption could be experimentally measured in a non-invasive way. Due to the

349 uncertainty on the actual values of these parameters and to the fact that they have a similar
350 effect on the air flow rate (Eq. 5), the volume variation of the oral cavity during the
351 consumption of cheese was arbitrarily fixed to a reference value of 20% of the mean volume
352 and the opening frequency of the velopharynx was a degree of freedom of the model.

353 The contact area between the liquid bolus and the product just before swallowing ($A_{OLPdeglu}$)
354 was calculated with the assumption of spherical particles:

$$355 \quad A_{OLPdeglu} = \frac{3 \times V_{OPini}}{R} \quad (25)$$

356 The particle radius R was estimated with a compression device designed by the Laboratoire
357 de Rhéologie (Grenoble, FRANCE) [26].

358 3.4. Air/bolus partition and mass transfer coefficients of aroma compounds in cheese bolus

359 The modification of the air/bolus partition coefficients of ethyl propanoate and 2-nonanone,
360 due to modification of the bolus composition, was determined by the static phase ratio
361 variation method (PRV) [27]. The mass transfer coefficients of aroma compounds into the
362 bolus were obtained by non-linear regression from dynamic headspace experiments
363 performed with Proton Transfer Reaction-Mass Spectrometry (PTR-MS) [7]. From those *in*
364 *vitro* measurements, the relationships describing the modifications of air/bolus partition and
365 the mass transfer coefficients of ethyl propanoate and 2-nonanone in bolus as a function of
366 cheese/saliva mass ratio were integrated into the model. The cheese/saliva mass ratio r_{cs} used
367 in the equations is given by:

$$368 \quad r_{cs} = \frac{V_{OPD}}{V_{OPD} + V_{OS}} \quad (26)$$

369 3.5. Estimation of cheese dissolution rate in artificial saliva

370 Considering the previously mentioned assumption of product dissolution, the dissolution rate
371 was estimated from measurements of the release of ionic species into warm artificial saliva,
372 using a conductivity probe. This measurement was chosen for its simplicity and for the
373 possibility to perform on-line measurements. The release of salts is considered here as a

374 marker of the matrix dissolution. The conductivity probe was calibrated at 35°C, with
375 aqueous NaCl solutions prepared with deionised water. Concentrations were measured in g/L
376 NaCl equivalent. A 6g-cylinder of cheese matrix, cut with a 24-mm punch, was placed in a
377 beaker containing 400 ml of artificial saliva (including 0.216 g of mucin (from porcine
378 stomach type II, SIGMA-ALDRICH) per 100g) and a magnetic stirrer. The monitoring of salt
379 release (actually all species contributing to the conductivity signal) was made during two
380 minutes using a conductivity meter (MPC HEITOLAB 350) and a probe (DCP 4). Product
381 dissolution rate was determined by nonlinear regression using Matlab 7 (Natick, MA), using
382 Eq. 27.

$$383 \quad \phi_{salt}(t) = v \times A(t) \times (C_{P_{salt}} - C_{S_{salt}}(t)) \quad (27)$$

384 where ϕ_{salt} is the salt mass flux between the product and saliva, $A(t)$ the product/saliva contact
385 area and $C_{P_{salt}}$ and $C_{S_{salt}}$ the salt concentrations in the solid product and in artificial saliva
386 respectively.

387 3.6. Measurements of aroma compound retention by lubricated mucosa using Proton Transfer 388 Reaction-Mass Spectrometry (PTR-MS)

389 Flavoured solutions were prepared with mineral water (Evian), ethyl propanoate and 2-
390 nonanone (final concentration of 4.8mg/L for each). 134.8cm³ Schott vials, equipped with
391 caps fitted with two valves (Interchim SCAT or InterchimOmnifit, England), were half-filled
392 with flavoured solutions and left at 35°C for 2 h to allow thermal equilibrium.

393 Five panelists were recruited for this specific measurement and were instructed to suck up a
394 mouthful of vial headspace with a straw, to swallow it and to continue to breathe normally
395 through the nose. A minimum of three replicates was performed for each individual. During
396 this experiment, the dynamic release of aroma compounds was measured online using Proton
397 Transfer Reaction Mass Spectrometry (PTR-MS, Ionicon Analytik, Innsbruck, Austria). The
398 PTR-MS inlet was connected to the subject's nose *via* a 1/16" PEEK tube maintained at 60°C.

399 Air was sampled from the subject's nose at a flow rate of 35 cm³/min *via* two inlets of a
400 stainless nosepiece placed in both of the assessor's nostrils. The PTR-MS instrument drift tube
401 was thermally controlled ($T_{\text{drift}}=60^{\circ}\text{C}$) and operated at $P_{\text{drift}}=200$ Pa with a voltage set of
402 $U_{\text{drift}}=600$ V. Measurements were performed with the multiple ion detection mode on specific
403 masses with a dwell time per mass of 50 ms. Ethyl propanoate and 2-nonanone were
404 respectively monitored at m/z 103 (molecular ion) and m/z 143 (molecular ion). In addition,
405 m/z 59 (acetone) was monitored as a breath marker and m/z 21 (signal for $\text{H}_3^{18}\text{O}^+$) and m/z 37
406 (signal for water clusters $\text{H}_2\text{O}-\text{H}_3\text{O}^+$) were monitored to check the instrument performances
407 and cluster ion formation.

408 3.7. Statistical analysis

409 Due to the small size and the non-normal characteristic of the dataset, classical analysis of
410 variance was not appropriate (univariate procedure using SAS/Stat® software). Instead,
411 Friedman tests were performed with an Excel program (available at www.Anastats.fr).
412 Rankings of samples were then obtained by the non-parametric test of multiple comparisons
413 (Bonferroni method, level of significance set at 5%). For the correlation test, the Spearman
414 test was performed, with a level of significance set at 5% (www.Anastats.fr).

415 4. Results and Discussion

416 4.1. Model simulations: insights in non-measured variables and assumptions on governing 417 mechanisms

418 Figure 3 shows the time variation of 9 out of the 15 model variables for the release of ethyl
419 propanoate during consumption of the cheese matrix FFl. Values of physiological parameters
420 were fixed to the panel mean.

421 The volume of product present in the mouth V_{OP} decreases slightly during the chewing period
422 before swallowing due to dissolution phenomenon (figure 3.a). Then, it decreases sharply at
423 the moment of swallowing. After that, only a small product portion remains in the mouth. The

424 main phenomenon responsible for product volume variations appears to be the swallowing
425 event, the dissolution having only a minor contribution. The change in saliva volume in
426 mouth V_{OS} is dependent on the rate of saliva incorporation in the liquid phase of the bolus
427 Q_{OS} (assumed constant) (figure 3.b). Therefore, the longer the chewing period before
428 swallowing, the larger this volume is. Each swallow brings the volume of saliva in the mouth
429 down to the baseline. The volume of product dissolved in the liquid phase of the bolus V_{OPD}
430 (figure 3.c) has a minor contribution in the total volume of the liquid phase of the bolus V_{OL} ,
431 compared to the volume of incorporated saliva V_{OS} .

432 The contact area between the solid and liquid phases of the bolus in the mouth A_{OLP} increases
433 rapidly before the first swallow because of product fragmentation during the chewing process
434 (figure 3.d). Then, the contact area decreases sharply at swallowing. Its variation between
435 secondary swallows is small, because of the small amount of product remaining in the mouth.
436 The concentration of aroma compounds in the air in the oral cavity C_{OA} increases until
437 swallowing due to mass transfer from the liquid bolus to the air (figure 3.e). The velopharynx
438 opening causes small cyclical depressions. Then, swallowing creates a renewal of air and
439 therefore a sharp decrease in concentration. Before the first swallowing, the concentration of
440 aroma compound in the liquid phase of the bolus C_{OL} increases due to the supply of aroma
441 compounds from product (figure 3.f). This increase is promoted by a large contact area
442 between the solid product and the liquid bolus. After swallowing, little product remains in the
443 mouth; the transfer of aroma compound to the air and saliva dilution become dominant, which
444 explain the overall decrease in aroma compound concentration in the liquid phase of the
445 bolus. Globally, the change in concentration of aroma compounds in the air in the oral cavity
446 C_{OA} follows the concentration in the liquid phase of the bolus C_{OL} . The concentration of
447 aroma compounds in the pharyngeal deposit C_{FL} is null during the consumption stage
448 preceding the first swallow (figure 3.g). After swallowing, a portion of the liquid fraction of

449 the bolus is deposited in the pharynx, which causes a sharp increase in the concentration.
450 Then, aroma compounds in the pharyngeal deposit are gradually released to the air phase.
451 During secondary swallowing events, the deposit is renewed by the food bolus coming from
452 the oral cavity. However, the new layer is already depleted in aroma compounds, which leads
453 to a general decrease in C_{FL} . The air in the pharynx (C_{FA}) receives aroma compounds from
454 the pharyngeal deposit and from the air of the oral cavity at each velopharynx opening (minor
455 peaks observed on the curve) (figure 3.h). Overall, the kinetics of concentration in the
456 pharynx C_{FA} follow the one in oral cavity C_{OA} , up to a dilution factor. The concentration of
457 aroma compounds in the air in the nasal cavity C_{NA} evolves similarly to the one of the air in
458 the pharynx C_{FA} (figure 3.i). However, each inspiration of fresh air, which is aroma-free,
459 makes the signal of the concentration in the nasal cavity C_{NA} decrease to zero.

460 As illustrated in figure 3, modelling provided insight in the change in non measured variables.
461 An important outcome was an improved understanding of mechanisms governing aroma
462 release kinetics and of the underlying assumptions.

463 4.2.Comparison of model predictions with experimental data for ethyl propanoate

464 As no interaction with lubricated mucosa was assumed for ethyl propanoate, simulations were
465 performed using the model without lubricated mucosa compartment. To compare model
466 simulations with experimental *in vivo* release data for ethyl propanoate, the air flow rate
467 resulting from the frequency of velopharynx opening was adjusted to fit the simulated release
468 kinetics before the first swallowing. The rate of saliva incorporation into the food bolus was
469 also adjusted so that the simulated release kinetics after the first deglutition fitted the decay
470 phase of the experimental curve.

471 All simulations have been satisfactorily fitted to experimental data (the average error of the
472 model, for all cheeses and all individuals, was only $5.88\% \pm 2.81$). The two unknown

473 parameters of the model (the average rate of saliva incorporation into the bolus and the
474 frequency of velopharyngeal opening) could be estimated.

475 Figure 4 presents some comparisons of simulations and experimental data for panelists S001
476 and S101. We can observe that these two individuals present diversified consumption and
477 aroma release behaviours: for example, panellist S001 exhibits a consistently longer
478 mastication time before the first swallow than panellist S101, and both panellists have longer
479 mastication times for firm matrices, as one could expect. In spite of this diversity, the model
480 correctly described the *in vivo* release profiles. Some slight deviations can be noticed, as for
481 instance on figures 4.a and 4.b at about 10s and 30s respectively. A possible explanation
482 could be that individuals have more complex behaviour during food consumption than
483 currently assumed in the model; for example, the amplitude of jaw movement related to
484 parameter ΔV_{OA} in Eq. 5 may vary in the course of the mastication process. This cannot be
485 correctly represented by the model with constant values of physiological parameters. One
486 should also bear in mind that panellists' behaviour is not fully reproducible and the greyed
487 area in Figure 4 represents an interval of ± 1 standard deviation of 3 replicate experiments,
488 which is statistically expected to contain less than 58% of the data.

489 The mean rate of saliva incorporation into the bolus Q_{OS} (for all cheeses and all panelists),
490 experimentally determined using the percentage of saliva incorporated in the bolus and the
491 average chewing time, is 7.88 ± 4.39 mL/min (figure 5, bar B). Its value remains similar to the
492 one of Q_{OS} estimated by fitting simulations to experimental data (9.00 ± 3.65 mL/min, bar C
493 in figure 5). These values are also comparable (mean and standard deviation) to the salivary
494 flow values measured experimentally during food consumption by other authors [28-30].

495 Overall, the average rate of saliva incorporation into the bolus, either measured directly or
496 estimated by fitting simulations to experimental data, was statistically much higher than the
497 salivary flow measured with mechanical stimulation (9.00 ± 3.65 mL/min vs. 2.65 ± 0.87

498 mL/min, bar A in Figure 5) as already observed by Gavião *et al.* [25] (7.82±4.53 mL/min vs.
499 1.40±0.67 mL/min), meaning that the salivary flow obtained with a mechanical stimulus is
500 not representative of the actual one during product consumption.

501 When products are compared (table 1), it appears that the average rate of saliva incorporation
502 into the bolus for the cheese matrix Fh (firm with a high-fat content) is statistically lower than
503 for the others cheese matrices (2-fold factor between cheese matrix Fh and cheese matrices Sh
504 and FF1), probably due to a longest consumption duration of cheese matrix Fh, as already
505 observed in previous studies [23]. Indeed, the rate of incorporation of saliva into the bolus can
506 be expressed as: $Q_{OS} = \frac{\text{initial volume of saliva}}{\text{duration of consumption before swallowing}} + \text{salivary flow rate}$, with the initial
507 volume of saliva in mouth being the same whatever the consumption duration. If we assume
508 that the salivary flow rate is constant during time, it follows that the longer the consumption
509 duration, the smaller Q_{OS} will be. The presence of fat can also induce a decrease in salivary
510 flow, as already observed during the consumption of model cheese matrices [31]. In the
511 present study, it is likely that the low value of the average rate of saliva incorporation into the
512 bolus for the cheese matrix Fh is the result of the two phenomena mentioned above.

513 4.3. Comparison of model predictions with experimental data for 2-nonanone

514 *In vivo* observations highlighted that ethyl propanoate and 2-nonanone exhibit quite different
515 behavior in terms of persistence (figure 6): the release amount for 2-nonanone during phase 2
516 was systematically higher for all individuals and all cheese matrices than for ethyl propanoate
517 (significant difference between the areas under curve of the two aroma compounds, Friedman
518 and Bonferroni tests, $p < 0.05$, not shown). We assumed that this phenomenon was the result of
519 an interaction between this molecule and lubricated mucosa. A specific experiment, based on
520 swallowing of aromatized air, was performed to check this assumption (see Material and
521 Method section). An example of standardized release curve is shown in figure 7 for one
522 panelist. Statistical analysis confirmed that 2-nonanone (solid line) persists much longer than

523 ethyl propanoate (dotted line) in the exhaled air. This was observed for all panelists and all
524 replicates. Measurements by PTR-MS of the *in vitro* release of these two molecules by
525 diluting the headspace of a vial containing the same aqueous flavoured solution excluded a
526 retention effect of the PTR-MS transfer line. All these results confirmed the existence of a
527 significant retention of the 2-nonanone by oral, pharyngeal and/or nasal lubricated mucosa.
528 This phenomenon has already been highlighted for other volatile compounds such as ethanol
529 or menthol [4, 32].

530 Simulations performed with the model including lubricated mucosa compartments were
531 compared to *in vivo* release data for 2-nonanone for cheese matrices FFI and SI. No data was
532 available for the two others cheese matrices since 2-nonanone was not detected because of its
533 high hydrophobicity and of retention by fat. The frequency of velopharynx opening and the
534 rate of saliva incorporation into the food bolus which were previously found for ethyl
535 propanoate were kept identical. Results showed that all simulations satisfactorily fitted
536 experimental data if a mucosa layer thickness of 100 μm and a transfer coefficient of
537 $1 \times 10^{-1} \text{cm/s}$ were fixed for all individuals (figure 8). The average error of the model was
538 $13.16\% \pm 6.80$, for the two cheese matrices tested and for the ten individuals. These results will
539 have to be refined in the future, through dedicated experiments to measure aroma compound
540 retention by lubricated mucosa.

541 4.4. Velopharynx opening

542 The results of the model fitting suggested that velopharynx opening can be different between
543 individuals. We found that in 53% of cases, the velopharynx opening was synchronized with
544 chewing frequency; in 37% of cases, it was synchronized with respiratory frequency and in
545 the 10% remaining cases, subjects had an intermediate behavior. Although little data is
546 available on this topic in the literature, these results are consistent with observations from
547 Matsuo *et al.* [18], who studied the velopharynx opening of 9 persons by videofluorography

548 during the consumption of various foods (banana, cookie, meat). They found that the opening
549 frequency varied widely among subjects, but that the opening time was related to jaw
550 movements. A link between breathing and velopharynx movements was also highlighted.

551 4.5. Analysis of model sensitivity

552 An analysis of model sensitivity was performed to evaluate the effect of some physiological
553 or physicochemical parameters on the variation of nasal concentration with time. A standard
554 nasal concentration curve was determined using mean values for panellist characteristics.
555 Then, each parameter was multiplied or divided by a factor of two (which is representative of
556 the typical variability of physiological parameters).

557 To assess the effect of each parameter on release intensity, each simulated kinetic was scaled
558 by the maximum of the standard nasal concentration curve. Three parameters were found to
559 have a strong positive effect on release intensity: the product dissolution rate in the mouth, the
560 mass transfer coefficient of aroma compound in the bolus and the air-bolus contact area in the
561 mouth. The respiratory frequency had a significant negative effect on nasal aroma
562 concentration by increasing aroma compound removal.

563 To assess the effect of each parameter on release dynamics, independently from global
564 intensity, each simulated kinetic was scaled by its own maximum intensity. Results showed
565 that only three out of the twenty parameters of the model had a major influence on the overall
566 kinetics (results not shown): the rate of saliva incorporation into the bolus during food
567 consumption Q_{OS} , the duration of the mastication before the first swallowing and the
568 velopharynx opening (amplitude ΔV_{OA} and frequency $fr_{opening}$). For example, an increase in
569 the rate of saliva incorporation into the bolus during food consumption resulted in a decrease
570 in the nasal concentration after the first swallow, due to the renewal of liquid phases present
571 in the mouth and pharynx (supply of fresh saliva). These results from sensitivity analysis and
572 the high level of uncertainty and of variability among individuals for physiological parameters

573 explained why the rate of saliva incorporation into the bolus during food consumption Q_{OS}
574 and the frequency of the velopharynx opening $fr_{opening}$ were selected as the two degrees of
575 freedom of the model.

576 **5. Conclusions**

577 In conclusion, it appears that the proposed model adequately simulated ethyl propanoate
578 release during the consumption of masticated matrices by a panel of ten individuals. The
579 estimation of the average rate of saliva incorporation into the bolus and the frequency of
580 velopharyngeal opening were in agreement with literature data. This study pointed out the
581 role of mastication on the release of aroma compounds during consumption of solid food, by
582 notably impacting the residence time of products in mouth and the opening of velopharynx
583 during product intra-oral manipulation, which ensures a continuous supply of aroma
584 compounds in the nose. Model sensitivity analysis highlighted that the parameters having a
585 major impact on flavour release when eating a solid food product are partly different from the
586 ones highlighted in the case of liquid or semi-liquid food [7]: in that case, the mass transfer
587 coefficient in the bolus, the breath flow rate and the thickness of post-deglutition pharyngeal
588 residue were the three key factors governing the release of aroma compounds. Differences
589 with previous work on liquid and semi-liquid food products mainly come from the duration of
590 food residence in the mouth.

591 The release of 2-nonanone highlighted the existence of retention phenomenon of this
592 molecule by lubricated mucosa. The model successfully accounted for this phenomenon.
593 Further work could help clarifying the binding mechanisms and come up with a satisfactory
594 quantitative description of the retention phenomenon [33, 34].

595 Overall, experimental release studies combined with mechanistic modelling help gaining new
596 insight into the complex phenomena of *in vivo* aroma compound release during the

597 consumption of a solid food, by understanding the relative contributions of product properties,
598 of individual characteristics and of their interactions.
599

600 **Nomenclature**

Symbol	Unit	Parameter
A	cm ²	Product/saliva contact area
A _{FAL}	cm ²	Air/liquid bolus contact area in the pharynx
A _{OAL}	cm ²	Air/ liquid bolus contact area in the oral cavity
A _{NAM}	cm ²	Air/lubricated mucosa contact area in the nasal cavity
A _{OLP}	cm ²	Liquid bolus/product contact area in the oral cavity
C _{FA}	g/cm ³	Aroma concentration in the air in the pharynx
C _{FL}	g/cm ³	Aroma concentration in the liquid bolus in the pharynx
C [*] _{FL}	g/cm ³	Aroma concentration at the air/liquid bolus interface in the pharynx
C _{NA}	g/cm ³	Aroma concentration in the air in the nasal cavity
C _{NM}	g/cm ³	Aroma concentration in the lubricated mucosa in the nasal cavity
C _{OA}	g/cm ³	Aroma concentration in the air in the oral cavity
C [*] _{OAL}	g/cm ³	Aroma concentration at the air/ liquid bolus interface in the oral cavity
C _{OL}	g/cm ³	Aroma concentration in the liquid bolus in the oral cavity
C _{OP}	g/cm ³	Aroma concentration in the product in the oral cavity
C _{P_salt}	g/cm ³	Salt concentration in the solid product
C _{S_salt}	g/cm ³	Salt concentration in artificial saliva
C _{TA}	g/cm ³	Aroma concentration in the trachea
E	cm	Residual bolus layer thickness in the pharynx
e _{NM}	cm	Layer thickness of the lubricated mucosa in the nasal cavity
F _R	Number of cycles/s	Respiratory frequency
fr _{masticatory}	Number of chews/s	Masticatory frequency
fr _{opening}	Occurrence number/s	Opening frequency of the velopharynx
HM _{bolus}	%	Moisture content of the bolus
HM _{cheese}	%	Moisture content of cheese product
K _{FAL}		Air/ liquid bolus partition coefficient in the pharynx

K_{NAM}		Air/ mucosa partition coefficient in the nasal cavity
K_{OAL}		Air/ liquid bolus partition coefficient in the oral cavity
k_{FL}	m/s	Mass transfer coefficient in the liquid bolus in the oral pharynx
k_{NM}	m/s	Mass transfer coefficient in the lubricated mucosa in the nasal cavity
k_{OA}	m/s	Mass transfer coefficient in the air phase in the oral cavity
k_{OL}	m/s	Mass transfer coefficient in the liquid bolus in the oral cavity
R	m	Average radius of particles in the bolus.
r_L	g/g	Mass fraction of liquid bolus remaining in the mouth after deglutition
r_{cs}	g/g	Cheese/saliva mass ratio
t_{deg}	s	Swallowing moment
Q_{NA}	cm ³ /s	Air flow rate coming from the nasal cavity
Q_{OA}	cm ³ /s	Air flow rate coming from the oral cavity
Q_{OS}	cm ³ /s	Average rate of saliva incorporation in the bolus
Q_{TA}	cm ³ /s	Air flow rate coming from the trachea
v	cm/s	Product dissolution rate in the saliva
V_{FA}	cm ³	Volume of air in the pharynx
V_{FL}	cm ³	Volume of liquid bolus in the pharynx
V_{lung}	cm ³	Lung volume
V_{NA}	cm ³	Volume of air in the nasal cavity
V_{NM}	cm ³	Volume of lubricated mucosa in the nasal cavity
V_{OA}	cm ³	Volume of air in the oral cavity
ΔV_{OA}	cm ³	Amplitude of mouth volume variation during mastication
V_{OL}	cm ³	Volume of liquid bolus in the oral cavity
V_{OP}	cm ³	Volume of product in the oral cavity
V_{OPD}	cm ³	Volume of dissolved product in the bolus of the oral cavity
V_{OS}	cm ³	Volume of saliva in the bolus

$V_{Salivadeq+}$	cm^3	Volume of saliva usually present in the oral cavity after swallowing
V_T	cm^3	Tidal volume
ϕ_{FAL}	g/s	Volatile mass flux between the air and the liquid bolus in the pharynx
ϕ_{NAM}	g/s	Volatile mass flux between the air and lubricated mucosa in the nasal cavity
ϕ_{OAL}	g/s	Volatile mass flux between the air and the liquid bolus in the oral cavity
ϕ_{salt}	g/s	Salt mass flux between the product and saliva
τ	s	Characteristic time of the aroma release decay

601 Remark: The solid part of the bolus consists of the non-dissolved part of the food product.

602 **Acknowledgements**

603 The authors gratefully acknowledge the French National Research Agency (ANR) project

604 “SensInMouth” for financial support.

605

606

607 **References**

- 608 [1] Chen, J. S. Food oral processing - a review. *Food Hydrocolloids*, **2009**, 23(1), 1-25.
- 609 [2] Harrison, M., B. P. Hills, J. Bakker and T. Clothier. Mathematical models of flavor release
610 from liquid emulsions. *Journal of Food Science*, **1997**, 62(4), 653-664.
- 611 [3] Overbosch, P., W. G. M. Afterof and P. G. M. Haring. Flavor release in the mouth. *Food*
612 *Review International*, **1991**, 7, 137.
- 613 [4] Normand, V., S. Avison and A. Parker. Modeling the Kinetics of Flavour Release during
614 Drinking. *Chemical Senses*, **2004**, 29(3), 235-245.
- 615 [5] Wright, K. M. and B. P. Hills. Modelling flavour release from a chewed bolus in the
616 mouth: Part II. The release kinetics. *International journal of Food Science and*
617 *Technology*, **2003**, 38(3), 361-368.
- 618 [6] Tréléa, I. C., S. Atlan, I. Déléris, A. Saint-Eve, M. Marin and I. Souchon. Mechanistic
619 mathematical model for in vivo aroma release during eating of semi-liquid foods.
620 *Chemical Senses*, **2008**, 33(2), 181-192.
- 621 [7] Doyennette, M., C. De Loubens, I. Déléris, I. Souchon and I. C. Tréléa. Mechanisms
622 explaining the role of viscosity and post-deglutitive pharyngeal residue on in vivo aroma
623 release: A combined experimental and modeling study *Food Chemistry*, **2011**, 128(2),
624 380-390.
- 625 [8] Harrison, M., S. Campbell and B. P. Hills. Computer simulation of flavor release from
626 solid foods in the mouth. *Journal of Agricultural and Food Chemistry*, **1998**, 46(7),
627 2736-2743.
- 628 [9] de Roos, K. B. and K. Wolswinkel. *Non-equilibrium partition model for predicting*
629 *flavour release in the mouth*. Elsevier Science, **1994**.
- 630 [10] Hills, B. P. and M. Harrison. Two-film theory of flavour release from solids.
631 *International journal of Food Science and Technology*, **1995**, 30, 425-436.

- 632 [11] Peyron, M. A., A. Mishellany and A. Woda. Particle Size Distribution of Food Boluses
633 after Mastication of Six Natural Foods. . *Journal of Dental Research*, **2004**, 83(7), 578-
634 582.
- 635 [12] Tobitsuka, K., M. Miura and S. Kobayashi. Retention of a European Pear Aroma Model
636 Mixture Using Different Types of Saccharides. *Journal of Agricultural and Food*
637 *Chemistry*, **2006**, 54, 5069-5076.
- 638 [13] Agrawal, K. R., P. W. Lucas, J. F. Prinz and I. C. Bruce. Mechanical properties of foods
639 responsible for resisting food breakdown in the human mouth. *Archives of Oral Biology*,
640 **1997**, 42(1), 1-9.
- 641 [14] van der Bilt, A., L. W. Olthoff, H. W. van der Glas, K. van der Weelen and F. Bosman.
642 A mathematical description of the comminution of food during mastication in man.
643 *Archives of Oral Biology*, **1987**, 32(8), 579-586.
- 644 [15] Wright, K. M. and B. P. Hills. Modelling flavour release from a chewed bolus in the
645 mouth: Part I. Mastication. *International Journal of Food Science and Technology*, **2003**,
646 38(3), 351-360.
- 647 [16] de Loubens, C., M. Panouillé, A. Saint-Eve, I. Déléris, I. C. Tréléa and Souchon I. .
648 Mechanistic model of in vitro salt release from model dairy gels based on standardized
649 breakdown test simulating mastication. *Journal of Food Engineering* **2011**, 105(1), 161-
650 168.
- 651 [17] Cussler, E. L. *Diffusion. Mass Transfer in Fluid Systems*. University Press, Cambridge,
652 **1997**.
- 653 [18] Matsuo, K., H. Metani, K. A. Mays and J. B. Palmer. Effects of Respiration on Soft
654 Palate Movement in Feeding. *Journal of Dental Research*, **2010**, 89, 1401-1406.

- 655 [19] Doyennette, M., I. Déléris, A. Saint-Eve, A. Gasiglia, I. Souchon and I. C. Tréléa. The
656 dynamics of aroma compound transfer properties in cheeses during simulated eating
657 conditions. *Food Research International*, **2011**, 44(10), 3174-3181.
- 658 [20] Levitzky, M. G. *Pulmonary physiology*, **2003**.
- 659 [21] Hornung, D. E., S. L. Youngentob and M. M. Mozell. Olfactory Mucosa-Air Partitioning
660 of Odorants. *Brain Research Bulletin.*, **1987**, 413(1), 147-154.
- 661 [22] Shojaei, A. H. Buccal mucosa as a route for systemic drug delivery: a review. *Journal of*
662 *Pharmaceutical Sciences*, **1998**, 1(1), 15-30.
- 663 [23] Repoux, M., H. Laboure, P. Courcoux, I. Andriot, E. Semon, C. Yven, G. Feron and E.
664 Guichard. Combined effect of cheese characteristics and food oral processing on in vivo
665 aroma release. *Flavor and Fragrance Journal*, **2012**, 27(6), 414-423.
- 666 [24] Watanabe, S. and C. Dawes. A Comparison of the Effects of Tasting and Chewing Foods
667 On the Flow-rate of Whole Saliva In Man. *Archives of Oral Biology*, **1988**, 33, 761-764.
- 668 [25] Gaviao, M. B., L. Engelen and A. Van der Bilt. Chewing behavior and salivary secretion.
669 *European Journal of oral science*, **2004**, 112(1), 19-24.
- 670 [26] Yven, C., J. Patarin, A. Magnin, H. Labouré, M. Repoux, E. Guichard and G. Féron.
671 Consequences of individuals chewing strategies on bolus rheological properties at the
672 swallowing treshold. *Journal of Texture Studies*, **2012**, 43(4), 309-318.
- 673 [27] Etre, L. S., C. Welter and B. Kolb. Determination of gas-liquid partition coefficients by
674 automatic equilibrium headspace-gas chromatography utilizing the phase ratio variation
675 method. *Chromatographia*, **1993**, 35(1/2), 73-84.
- 676 [28] Mioche, L., O. Bourdiol, S. Monier and J. F. Martin. The relationship between chewing
677 activity and food bolus properties obtained from different meat textures. *Biosciences,*
678 *Biotechnology, Biochemistry*, **2002**, 69(9), 1669-1676.

- 679 [29] Patarin, J., D. Blésès, A. Magnin, C. Yven, H. Labouré and G. Féron. Mechanical
680 characterization of cheese food bolus: a new device. *Food Oral Processing congress*,
681 Leeds, U.K., **2010**.
- 682 [30] Anderson, K., G. S. Throckmorton, P. H. Buschang and H. Hayasaki. The effects of
683 bolus hardness on masticatory kinematics. *Journal of Oral Rehabilitation*, **2002**, 29(7),
684 689-696.
- 685 [31] Tarrega, A., C. Yven, E. Sémon and C. Salles. Aroma release and chewing activity
686 during eating different model cheeses. *International Dairy Journal*, **2008**, 18(8), 849-857.
- 687 [32] Van Ruth, S. M., J. Frasnelli and I. Carbonell. Volatile flavour retention in food
688 technology and during consumption: Juice and custard examples. *Food Chemistry*, **2008**,
689 106(4), 1385-1392.
- 690 [33] Medinsky, A. and J. A. Bond. Sites and mechanisms for uptake of gases and vapors in
691 the respiratory tract. *Toxicology*, **2001**, 160, 165-172.
- 692 [34] Kurtz, D. B., K. Zhao, D. E. Hornung and P. Scherer. Experimental and numerical
693 determination of odorant solubility in nasal and olfactory mucosa. *Chemical Senses*,
694 **2004**, 29(9), 763-773.
- 695 [35] Salles, C., M. C. Chagnon, G. Féron, E. Guichard, H. Labouré, M. Morzel, E. Sémon, A.
696 Tarrega and C. Yven. In-mouth mechanisms leading to flavor release and perception.
697 *Critical Reviews in Food Science and Nutrition*, **2011**.
- 698

699 **Figure captions**

700 Figure 1. Schematic representation of the chronological steps of the consumption of a solid
701 food product.

702 Figure 2. Schematic representation of the interconnected compartments and of the
703 mechanisms involved in flavour release during the consumption of a solid food product.

704 Figure 3. Time variation of 9 model variables for the release of aroma compounds during the
705 consumption of a solid product: (a) solid product volume in the mouth V_{OP} , (b) volume of
706 saliva in the mouth V_{OS} , (c) volume of dissolved product in the liquid phase of the bolus
707 V_{OPD} , (d) contact area between solid and liquid phases of the bolus in the mouth A_{OLP} , (e)
708 aroma compound concentration in the air of the oral cavity C_{OA} , (f) aroma compound
709 concentration in the liquid phase of the bolus in the mouth C_{OL} , (g) aroma compound
710 concentration in the pharyngeal deposit C_{FL} , (h) aroma compound concentration in the air in
711 the pharynx C_{FA} and (i) aroma compound concentration in the air in the nasal cavity C_{NA} .
712 Case of the consumption of the cheese matrix FFI and for ethyl propanoate, with typical
713 values of the physiological parameters. Time 0 corresponds to the moment of the first
714 swallowing. Vertical lines indicate the time of product introduction in mouth and the
715 successive swallowing events.

716 Figure 4. Comparison of simulated and experimental release profiles for ethyl propanoate for
717 panelists S001 (a-d) and S101 (e-h) and for cheese matrices FFI (a, e), Fh (b, f), Sl (c, g) and
718 Sh (d, h). For each figure, the simulation is represented by a thick line, the average curve of
719 the three replicates by a thin line and the envelope curve representing the standard deviation
720 of three repetitions by the "gray" area. The characteristic moments of consumption (product
721 introduction in mouth and the successive swallowing events) are represented by vertical lines.
722 The two graphs in the form of bars at the right of the main figure present the values of two
723 parameters before and after model fitting. The initial value is symbolized by a square and the

724 estimated value after the adjustment of the model by a triangle. The extreme values
725 (maximum and minimum) give the physiological range of variation for each parameter
726 (extracted from the initial panel of 50 individuals).

727 Figure 5. Comparison of the average rate of saliva incorporation into the bolus estimated by
728 model fitting with literature data. A) Salivary flow rate (parafilm stimulation), B) Average
729 rate of saliva incorporation in the bolus (determined experimentally by measuring the dry
730 extract of the bolus), C) Average rate of saliva incorporation in the bolus (estimated by model
731 fitting), D) Average rate of saliva incorporation in the bolus given by [25]), E) Average rate
732 of saliva incorporation in the bolus reported in [35]) and F) Average rate of saliva
733 incorporation in the bolus reported in [24]).

734 Figure 6. Comparison of *in vivo* release profiles of ethyl propanoate (thin envelope curve and
735 dark gray line) and 2-nonanone (thin envelope curve and light gray line) for subject S001,
736 cheese matrix FFI. The characteristic moments of consumption (product introduction in
737 mouth and the successive swallowing events) are represented by vertical lines.

738 Figure 7. Comparison of *in vivo* release of ethyl propanoate (dotted line) and 2-nonanone
739 (solid line) following the ingestion of flavoured air (1 panelist, 1 replicate). The data are
740 normalized to their maximum intensity.

741 Figure 8. Comparison of simulated and experimental release profiles for 2-nonanone for
742 panelist S001 for cheese matrices (a) FFI and (b) S1, and for panelist S101 for cheese matrices
743 (c) FFI and (d) S1. For each figure, simulation is represented by a thick line, the average curve
744 on the three replicates by a thin line and the envelope curve representing the standard
745 deviation of three repetitions by the "gray" area. The characteristic moments of consumption
746 (product introduction in mouth and successive swallowing events) are represented by vertical
747 lines.

748

749 **Table captions**

750 Table 1. Comparison of the average rates of saliva incorporation into the bolus (in mL/min)
751 for the 4 cheese matrices. The letters indicate the classification group of the products
752 (Friedman and Bonferroni tests are significant at the level 5%).

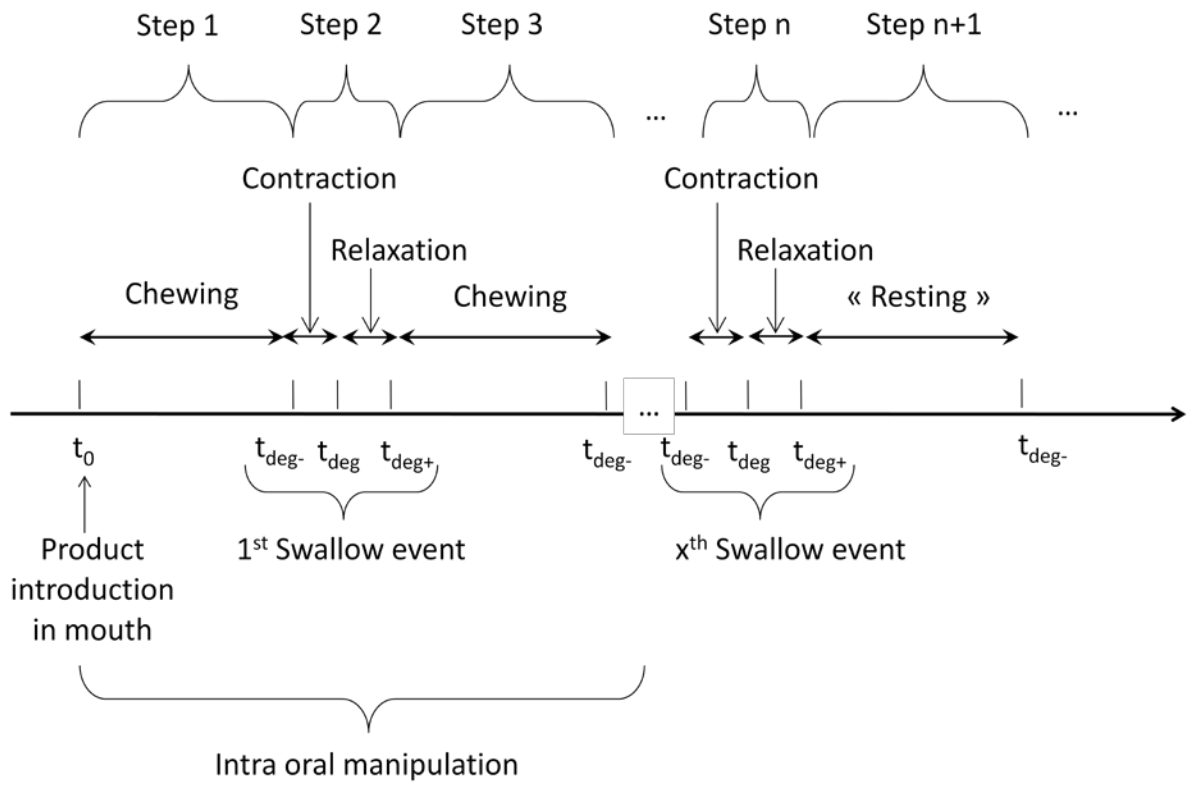


Figure 1.

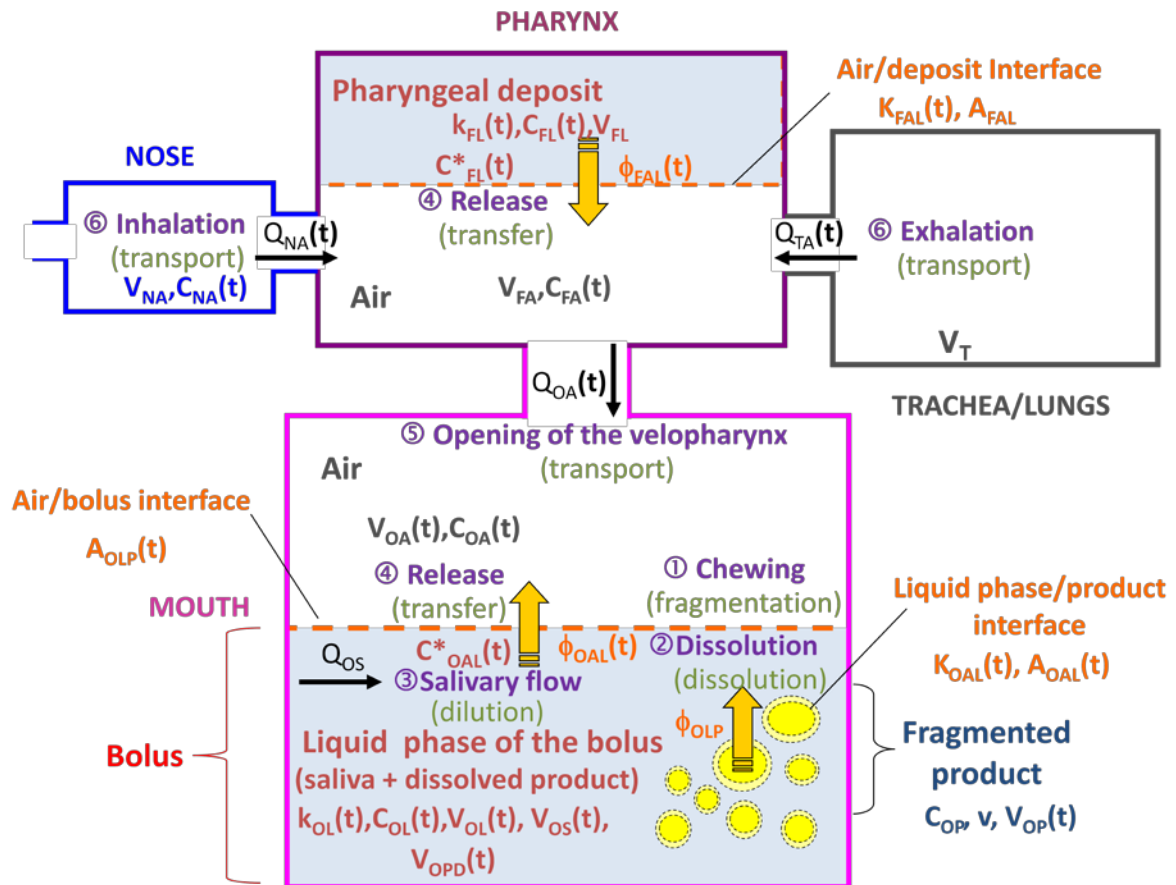


Figure 2.

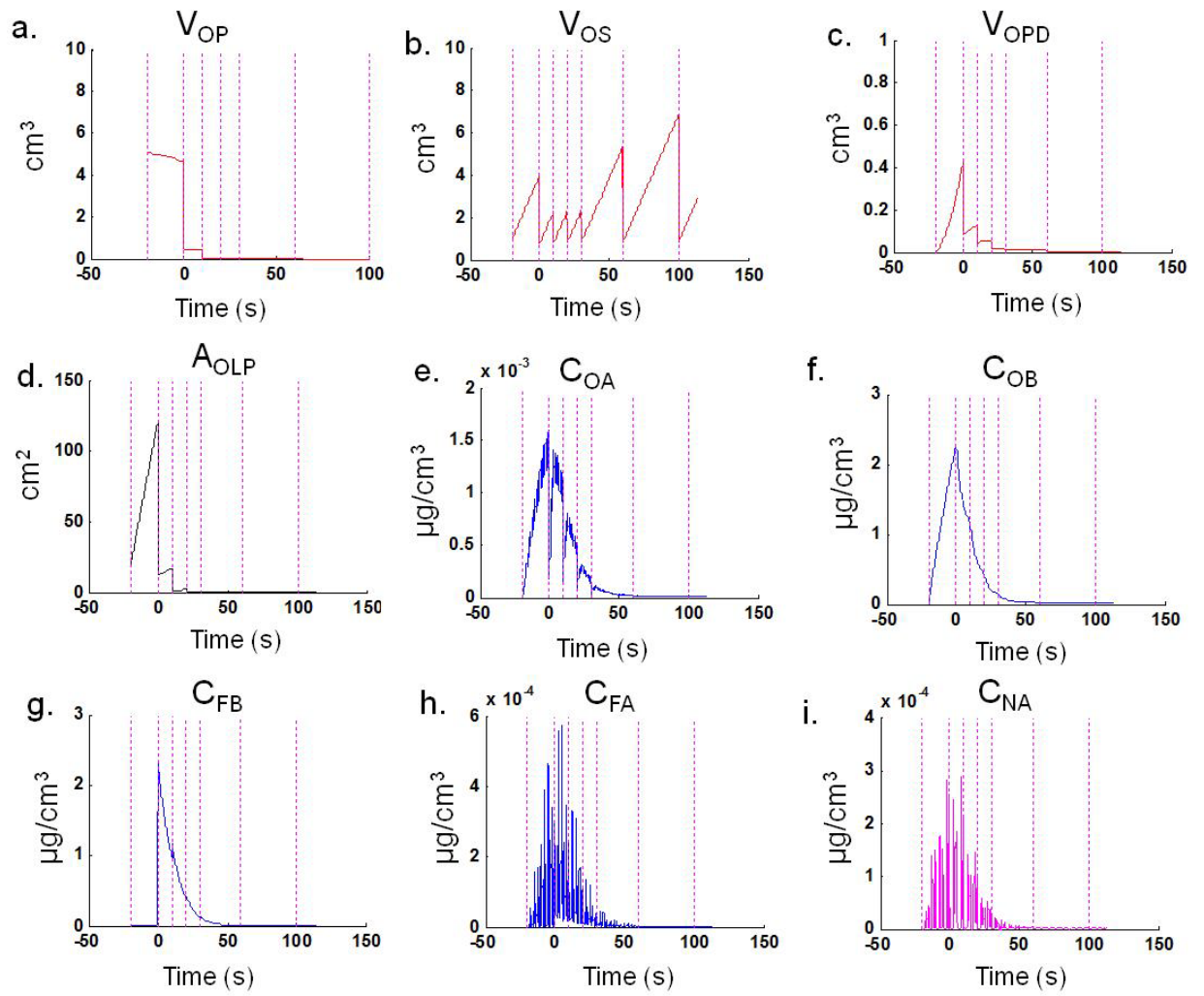


Figure 3.

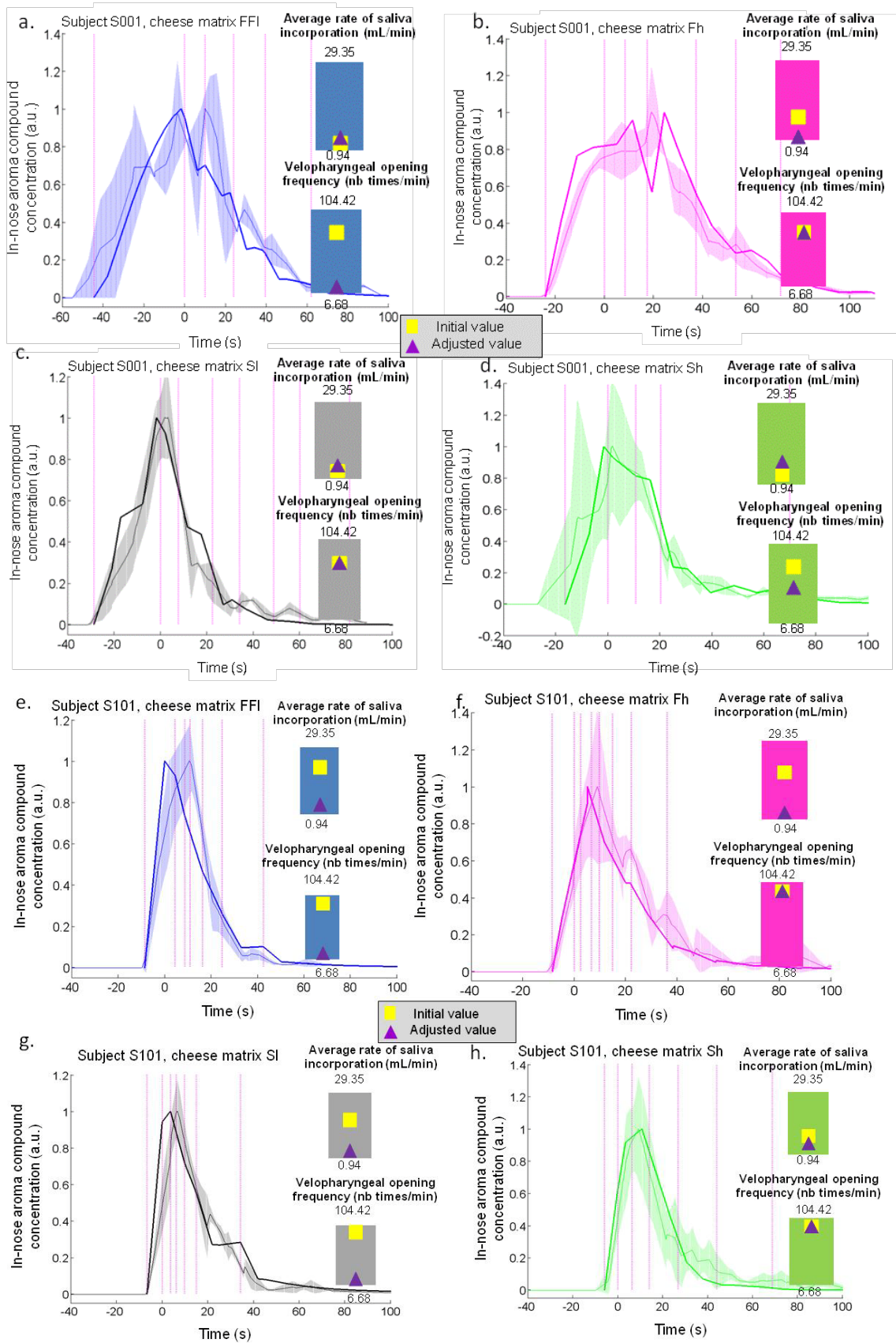


Figure 4.

4. Figure5

[Click here to download 4. Figure: Figure 5_doyennette.pdf](#)

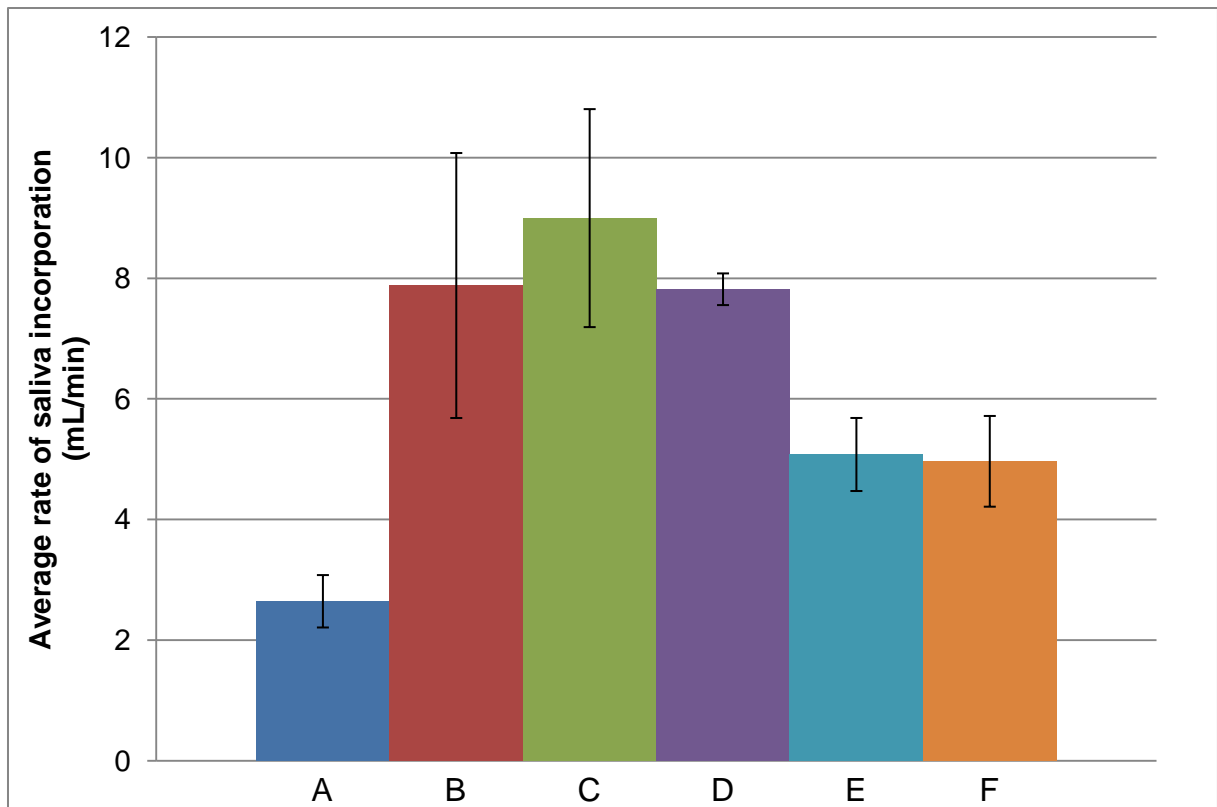


Figure 5.

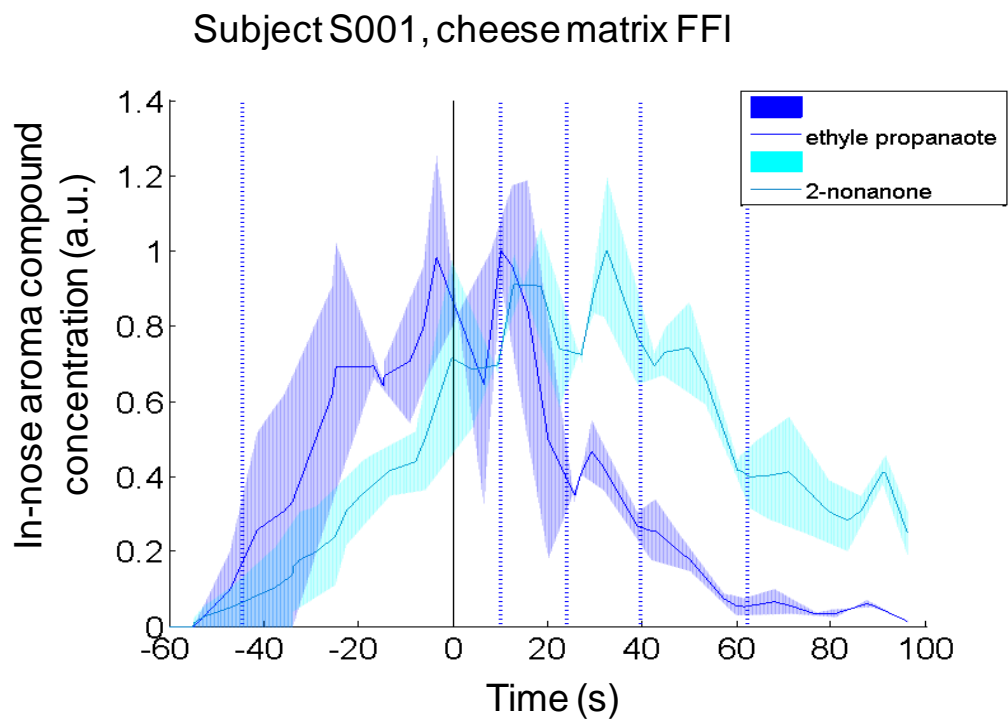


Figure 6.

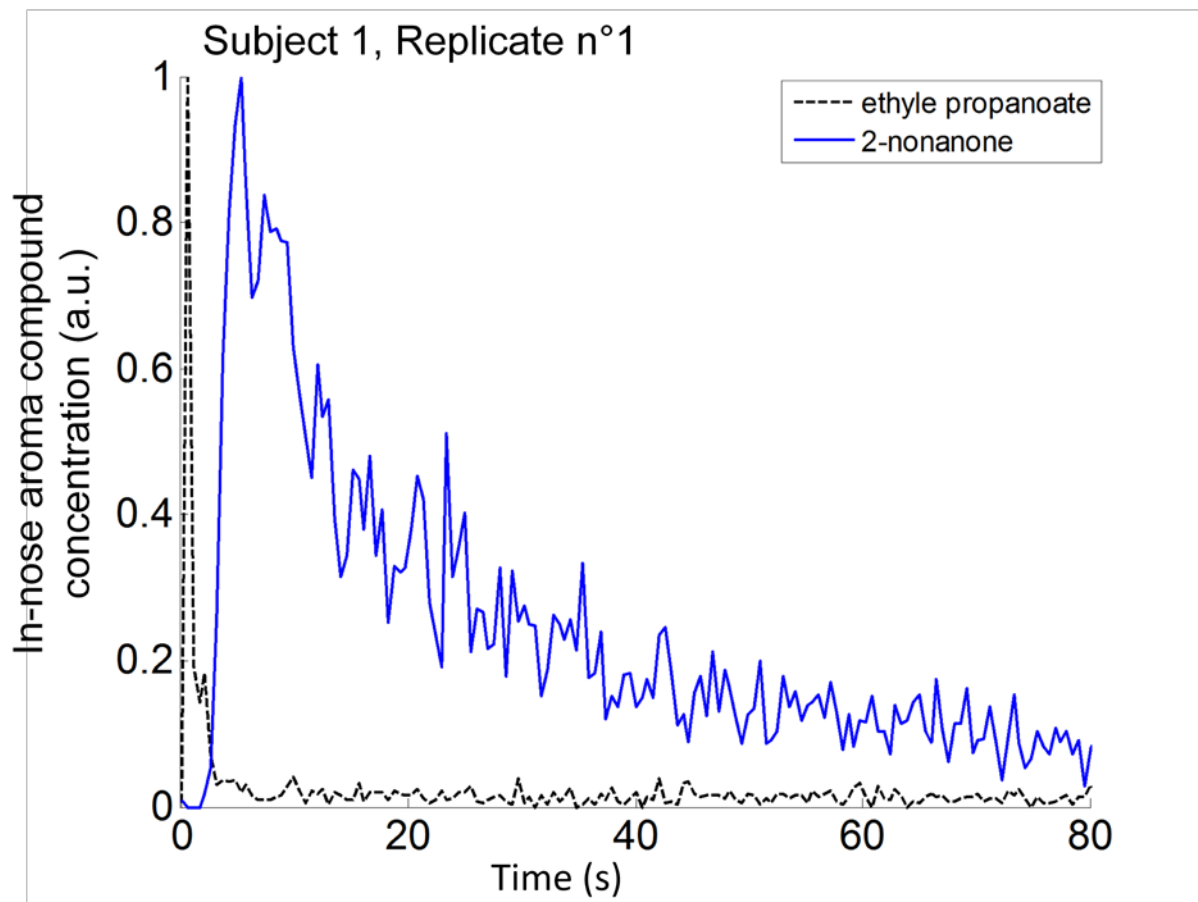


Figure 7

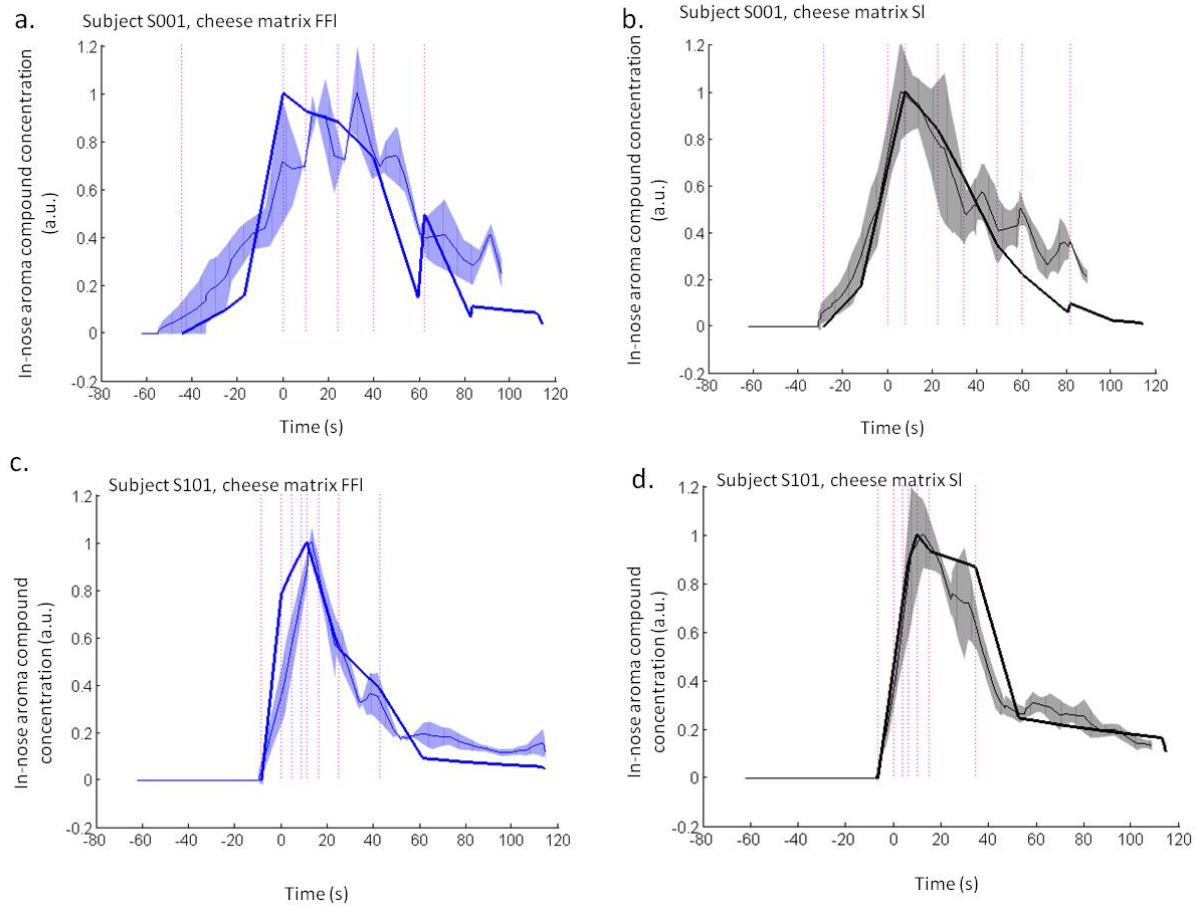


Figure 8

Table 1.

Rate of saliva incorporation	FFI	Sh	SI	Fh
Mean value (mL/min)	10.50	10.80	9.43	5.27
Standard deviation (mL/min)	5.70	4.97	6.16	8.08
Group	A	A	AB	B